NASA TECHNICAL NOTE

NASA TN D-6032

NASA TN D-6032

EVALUATION RESULTS AND ACCURACY IMPROVEMENT OF TWO FLUX-SWITCHING MATHEMATICAL MODELS FOR MAGNETIC CORES

by J. Larry Spencer

Langley Research Center
Hampton, Va. 23365

NATIONAL AERONAUTICS AND SPACE ADMINISTRATION • WASHINGTON, D. C. • NOVEMBER 1970

1. Report No.	2. Government Accession No.	3. Recipient's Catalog No.
NASA TN D-6032		

4. Title and Subtitle
EVALUATION RESULTS AND ACCURACY IMPROVEMENT OF TWO FLUX-SWITCHING MATHEMATICAL MODELS FOR MAGNETIC CORES

5. Report Date
November 1970

6. Performing Organization Code

7. Author(s)
J. Larry Spencer

8. Performing Organization Report No.
L-7300

9. Performing Organization Name and Address
NASA Langley Research Center
Hampton, Va. 23365

10. Work Unit No.
125-23-05-01

11. Contract or Grant No.

12. Sponsoring Agency Name and Address
National Aeronautics and Space Administration
Washington, D.C. 20546

13. Type of Report and Period Covered
Technical Note

14. Sponsoring Agency Code

15. Supplementary Notes

16. Abstract

The results of an evaluation of two flux-switching models for magnetic cores, the Nitzan model and the Betts and Bishop model, are presented. The two models are compared on the basis of the types of core switching each describes and the fidelity with which each predicts the output voltage waveform of a ferrite core with inside diameter of 50 mils (1.27 mm) and outside diameter of 80 mils (2.03 mm). The results indicate that the Nitzan model is more accurate and more nearly complete because it describes shuttling and partial switching. The Nitzan model is more applicable to cores of the same material but different sizes because it uses separate parameters related to the core materials and the core dimensions. A method is presented by which both models can be extended to describe more accurately the switching of cores with smaller ratios of inside to outside diameter.

17. Key Words (Suggested by Author(s))	18. Distribution Statement
Mathematical magnetic core models Flux-switching models	Unclassified – Unlimited

19. Security Classif. (of this report)	20. Security Classif. (of this page)	21. No. of Pages	22. Price*
Unclassified	Unclassified	32	$3.00

*For sale by the Clearinghouse for Federal Scientific and Technical Information
Springfield, Virginia 22151

EVALUATION RESULTS AND ACCURACY IMPROVEMENT OF TWO FLUX-SWITCHING MATHEMATICAL MODELS FOR MAGNETIC CORES

By J. Larry Spencer
Langley Research Center

SUMMARY

The results of an evaluation of two flux-switching models for magnetic cores, the Nitzan model and the Betts and Bishop model, are presented. The two models are compared on the basis of the types of core switching each describes and the fidelity with which each predicts the output voltage waveform of a ferrite core with inside diameter of 50 mils (1.27 mm) and outside diameter of 80 mils (2.03 mm). The results indicate that the Nitzan model is more accurate and more nearly complete because it describes shuttling and partial switching. The Nitzan model is more applicable to cores of the same material but different sizes because it uses separate parameters related to the core materials and the core dimensions. A method is presented by which both models can be extended to describe more accurately the switching of cores with smaller ratios of inside to outside diameter.

INTRODUCTION

For the mathematical analysis and design of magnetic core circuits, it is necessary to have a mathematical model to describe the operation of a magnetic core. A flux-switching model for a magnetic core describes mathematically the output voltage-time waveforms appearing on the sense winding as a function of the current through the drive winding. A core model for use in circuit analysis and design should accurately predict the output voltage of a core under all switching conditions but be simple enough to aid the designer of magnetic circuits.

Most of the existing core models are based on an approach developed by Menyuk and Goodenough (ref. 1), which predicts the output voltage on the sense winding as a function of the input current and initial flux state of the core. Seven flux-switching models for magnetic cores were evaluated by Hesterman (ref. 2), who concluded that the linear parabolic flux-switching model is the best for fast switching and the nonlinear parabolic model is the best for slow switching. Nitzan et al. (refs. 3 to 10) combined the linear and nonlinear parabolic models and extended the model to describe shuttling and incomplete

switching. In Hesterman's report, reference 2, a model developed by Betts and Bishop (ref. 11) was listed as promising, but the model was not evaluated. In the present study the models developed by Betts and Bishop and by Nitzan are compared and evaluated. These models describe switching of a magnetic core from the maximum or minimum residual-flux level. A method is also presented for improving the accuracy of both models in predicting the output voltage of a "thick" core. The symbols used are defined in appendix A and a brief description of the models is presented in appendix B.

COMPARISON OF THE MODELS

The Betts and Bishop model and the Nitzan model are of a complexity that dictates their solution on a computer. The computer times for the two models are nearly equal, and therefore the speed of solution is not a factor in their comparison. The two models are compared first on the basis of the types of core switching each describes and then on the basis of the accuracy with which each model predicts the output voltage of a core. A typical hysteresis loop for a magnetic core is shown in figure 1. The Betts and Bishop model describes only the complete switching ($\pm\Phi_r$ to $\mp\Phi_s$) of a magnetic core. The Nitzan model describes complete switching and also partial switching ($\pm\Phi_r$ to $\gtrless\mp\Phi_s$) because the static hysteresis loop and the nonlinear region of the peak output voltage curve are included in its parameters. The output voltage produced when the core is shuttled ($\pm\Phi_r$ to $\pm\Phi_s$) is predicted by the elastic switching part of the Nitzan model. The Nitzan model is more nearly complete than the Betts and Bishop model. Neither model will describe switching from a partially set state – that is, switching from some flux state other than $\pm\Phi_r$.

The accuracy of the models was studied by comparing the output voltage predicted by both models with the experimentally determined output voltage under the same drive conditions. Four different drive conditions were used. The ferrite core, which had an inside diameter of 50 mils (1.27 mm), an outside diameter of 80 mils (2.03 mm), and a height of 30 mils (0.76 mm), was completely switched by each drive condition. (This core is called the 50-80 core herein.) The test circuit shown in figure 2 was used to determine the experimental output voltage. The generator current waveform is shown in figure 3. The measurement of the experimental parameters for the models is described in detail in reference 12. Also in reference 12 is a complete set of computer programs in FORTRAN IV that describe the Nitzan model and the Betts and Bishop model. A CDC 6600 computer was used to obtain the predicted output voltage of the models for the accuracy comparison.

The voltage predicted by the models was compared with the experimentally obtained voltage for the following driving currents (pulse 1 in fig. 3):

Case	Current, I_{ss}, amperes	Rise time, t_{rise}, μsec
Ramp current switching	0.79	2.95
Ramp-step current switching	.77	.88
Slow step current switching	.79	.04
Fast step current switching	1.6	.035

Pulse 2 is used to reset the core. In ramp current switching the core is switched by a ramp driving current, whereas in ramp-step current switching the core is partially switched by a ramp and the switching is completed by a constant current. In slow step and fast step current switching the core is switched by a constant current having a very short rise time. The output voltage waveforms predicted by both models and the experimental output voltage waveform are shown in figures 4, 5, 6, and 7 for ramp, ramp-step, slow step, and fast step switching, respectively.

The Nitzan model describes the output voltage waveform for a core when partially switched. Figure 8 shows the waveform of the output voltage predicted by the Nitzan model and the experimental output of the 50-80 core when 11.5 maxwells (115 nanowebers) of the 12.6 maxwells (126 nanowebers) of flux is switched by a driving current of 0.4 ampere with a rise time of 0.04 microsecond. The Betts and Bishop model will not predict partial switching.

The Nitzan model also describes shuttling of the core. To apply the model to a shuttled core, the time rate of change of the applied current must be determined. The driving current was fitted by a polynomial as shown in figure 9. The equation of the driving current was differentiated with respect to time and multiplied by a core constant ϵ to obtain the prediction of the shuttling output voltage by the Nitzan model. The accuracy of the prediction is shown in figure 10.

EXTENSION OF THE MODELS

In figures 4 to 7 the calculated output voltage curves from both models are shifted to the right and up from the curve of the measured voltage. The models are more inaccurate when describing switching by a ramp driving current than by a step driving current. The main source of inaccuracy of the models for these particular tests is the assumption that the 50-80 core has a diametral ratio close to unity (thin). Restricting the models to thin cores justifies the assumption that the magnetic field intensity throughout the core material is a constant. The actual magnetic field intensity in a magnetic core is inversely proportional to the distance from the center of the core. In reference 13 the Betts and Bishop model was extended for cores of any diametral ratio by determining the output

voltage of a thin core in terms of the radius and analytically integrating this voltage from the inner to the outer radius of the core. The integration of the Betts and Bishop model complicates the model so that it cannot be used practically in circuit analysis.

By analytically dividing a thick core into concentric rings, where each ring can be assumed to be a thin core, and applying the thin-core model to each ring, the models are extended to describe switching of a thick core. The output voltage-time response of a thick core, as predicted by the extended models, is the analytical sum of the output voltage-time responses from each of the concentric rings. The two extended models, using two rings, were applied to the 50-80 core subject to the same test conditions as in figures 4 to 7. The results are shown in figures 11 to 14. (The scale changes on the time axis of the figures for the two-ring models result from the automatic plotting of the figures.) In all four cases, the accuracy of both models was improved. The greatest improvement exists for switching when the driving current is a ramp (compare figs. 4 and 11). By comparing the accuracies with which the models predict ramp switching and fast step switching in figures 4 and 7, respectively, it can be seen that what is considered to be a thin core for fast switching is a thick core for slow switching. In figure 11 the first peak in the output voltage waveform is caused by the domination of the faster switching, higher amplitude output voltage of the inner ring and the second peak is caused by the slower switching, lower amplitude output voltage of the outer ring. If more than two rings are used, the difference in the output voltages from the rings is less apparent in the sum. Therefore, the total output voltage obtained by summing the predicted output voltages of the rings is a smoother, more accurate prediction of the experimental output voltage of the core.

To prove that additional rings will improve the accuracy, a 10-ring Nitzan model was applied to ramp-current switching and partial switching, the two cases in which the one-ring model is most in error. Figure 15 shows the prediction of the output voltage for ramp-current switching with a 10-ring model. There is more improvement in the accuracy of the model in going from one to two rings than in going from two rings to 10 rings. The rings also improve the accuracy of the Nitzan model when describing incomplete switching. The Nitzan model for describing partial switching with 10 rings is shown in figure 16. The output voltage of a shuttled core as predicted by the Nitzan model is not affected by dividing the core into rings.

The percent of average deviation of the output voltage by the model from the experimental output voltage was calculated for both models under each driving current from the following equation:

$$\text{Percent average deviation} = \frac{\left| \int_0^{t_{sw}} \left[V_{o,exp}(t) - V_{o,m}(t) \right] dt \right|}{t_{sw} V_{o,p,exp}} \times 100$$

Table I gives the percentage of average deviation from the experimental output voltage for each case of complete switching and partial switching. The data show that for a particular core and a given drive condition, the accuracy of the models can be improved by using a larger number of rings to represent the thick core. However, the time required for computation increases in direct proportion to the number of rings used. Greater improvement is achieved with the first segmentation of the core into rings, and successive subdivisions result in less improvement.

TABLE I.- COMPARISON OF RESULTS FROM MODELS AND EXPERIMENT

Case	Percentage of average deviation from the experimental output voltage for –				
	Betts and Bishop model with –		Nitzan model with –		
	1 ring	2 rings	1 ring	2 rings	10 rings
Ramp current switching	44.8	31.5	22.5	11.7	11.1
Ramp-step current switching	22.1	17.9	12.1	7.3	Not tried
Slow step current switching	10.6	8.6	8.5	5.4	Not tried
Fast step current switching	6.9	6.4	7.1	6.7	Not tried
Partial switching	Not applicable		88	Not tried	13.5

CONCLUDING REMARKS

An evaluation of two flux-switching models for magnetic cores, the Betts and Bishop model and the Nitzan model, has been made. It is concluded that the Nitzan model is a more nearly complete model because it will describe shuttling and partial switching, whereas the Betts and Bishop model will not. Neither model will describe switching from a partially set state, which is an important switching condition in magnetic circuits. An advantage of the Nitzan model is that it uses one set of parameters related to the material of which the core is constructed and another set related to the physical dimensions of the core, whereas the Betts and Bishop model uses parameters of these quantities combined.

A method has been introduced for improving the accuracy of both models in predicting the output voltage of a "thick" core. It was found that the accuracy of both models in predicting the output voltage of a thick core is improved by accounting for the magnetic field intensity variation through the core. The extended models accounted for the field

variation by analytically segmenting the core into concentric rings and applying the model to each ring. The number of segmentations needed for accurate description of the output voltage is dependent upon the diametral ratio of the core, the driving current, and the squareness of the hysteresis loop of the core material.

Langley Research Center,
National Aeronautics and Space Administration,
Hampton, Va., September 4, 1970.

APPENDIX A

SYMBOLS

A	cross-sectional area of the core
B	magnetic flux density
$\dot{B}_p$	first derivative of peak flux density with respect to time
$\dot{B}_p(H)$	equation relating the peak flux density to the driving magnetic field intensity
B_r	maximum residual flux density
B_s	saturation flux density
C_n	coefficients of the characteristic equation for the Betts and Bishop model
$f(\tau)$	characteristic equation of normalized output voltage waveform
H	driving magnetic field intensity
H_{1-2}	magnetic field intensity boundary between region 1 and region 2 of the $\dot{B}_p(H)$ curve
H_{2-3}	magnetic field intensity boundary between region 2 and region 3 of the $\dot{B}_p(H)$ curve
H_a	magnetic field intensity asymptote for a parabola in describing the static B-H loop
H_{dyn}	dynamic magnetic field intensity threshold
H_{ext}	magnetic field intensity obtained by linearly extrapolating the $\dot{B}_p(H)$ curve to the H-axis
H_n	magnetic field intensity asymptote for a parabola in describing the static B-H loop

H_q magnetic field intensity at which the parabola in describing the static B-H loop intersects the $B = -B_s$ line

H_{st} static magnetic field intensity threshold

h axial dimension of the core

I amplitude of step driving current

I_{1-2} current boundary between region 1 and region 2 of the $\dot{\Phi}_p(I)$ curve

I_{2-3} current boundary between region 2 and region 3 of the $\dot{\Phi}_p(I)$ curve

I_{dyn} dynamic current threshold

I_{ext} current threshold obtained by linearly extrapolating the third region of the peak output voltage curve

I_i input driving current

I_{ss} steady-state driving current

I_{st} static current threshold

l magnetic path length

$\bar{l}$ mean magnetic path length, $\pi(r_i + r_o)$

l_i inside circumference of the core

l_o outside circumference of the core

R_p slope of peak output voltage curve

r_i inside radius of the core

r_o outside radius of the core

t time

t_p time at which peak output voltage occurs

t_{rise} rise time of the current

t_{sw} switching time

t_t time at which the driving current reaches the threshold of the core

$V_{o,exp}(t)$ experimental output voltage

$V_{o,m}$ output voltage predicted by a model

$V_{o,p}$ peak output voltage

$V_{o,p,exp}$ peak experimental output voltage

W_c core constant equal to $V_{o,p,exp}t_p$

δ coefficient of inelastic B

ϵ coefficient of elastic switching

κ_1 coefficient of inelastic B in nonlinear $\dot{B}_p(H)$ for $H_{st} \leqq H < H_{1-2}$

κ_2 coefficient of inelastic B in nonlinear $\dot{B}_p(H)$ for $H_{1-2} \leqq H < H_{2-3}$

λ_1 coefficient proportional to $\dot{\Phi}_p(I)$ for $I_{st} \leqq I < I_{1-2}$

λ_2 coefficient proportional to $\dot{\Phi}_p(I)$ for $I_{1-2} \leqq I < I_{2-3}$

ν_1 exponent of $\dot{\Phi}_p(I)$ for $I_{st} \leqq I < I_{1-2}$

ν_2 exponent of $\dot{\Phi}_p(I)$ for $I_{1-2} \leqq I < I_{2-3}$

ρ coefficient of inelastic $\dot{\Phi}$

τ normalized time, t/t_p

Φ magnetic flux

$\dot{\Phi}$	first derivative of flux with respect to time (voltage)
$\dot{\Phi}_{el}$	elastic portion of output voltage per turn of a core
$\dot{\Phi}_{inel}$	inelastic portion of output voltage per turn of a core
Φ_{max}	maximum flux switched, $\Phi_s + \Phi_r$
$\dot{\Phi}_p(I)$	equation relating the peak output voltage to the step driving current
Φ_r	maximum residual flux
Φ_s	saturation flux
$\Phi_{st}(I)$	equation of the static hysteresis loop

APPENDIX B

DESCRIPTION OF MODELS

The Betts and Bishop Model

The Betts and Bishop model mathematically predicts the output voltage of a thin square-loop magnetic core which is excited by a drive current. The Betts and Bishop model describes only complete switching of a core; that is, switching from $\pm\Phi_r$ to $\mp\Phi_s$, which means

$$\int_0^\infty V_{o,exp}(t)\,dt = \Phi_{max} = \text{Constant} \tag{1}$$

The Betts and Bishop model is based on two assumed conditions: (1) The open-circuit voltage-time waveforms caused by step input currents are identical when normalized with respect to peak amplitude and the time at which this occurs, and (2) the peak output voltage of an unloaded core is directly proportional to the magnitude of the step input current above the current threshold of the core I_{ext}. The normalized output voltage waveform is known as the characteristic curve, and the equation of this curve is the characteristic equation $f(\tau)$. The equation of the peak output voltage curve is

$$V_{o,p} = R_p(I - I_{ext}) \tag{2}$$

and the characteristic equation is

$$f(\tau) = \sum_{n=0}^{N} C_n \tau^n \tag{3}$$

The descriptive equations of the Betts and Bishop model for a step input current are

$$\left.\begin{aligned} V_{o,exp}(t) &= \begin{cases} 0 & (I < I_{ext}) \\ R_p(I - I_{ext})f(\tau) & (I \geq I_{ext}) \end{cases} \\ \tau &= \begin{cases} 0 & (I < I_{ext}) \\ \dfrac{R_p}{W_c}(I - I_{ext})t & (I \geq I_{ext}) \end{cases} \end{aligned}\right\} \tag{4}$$

where W_c is the product of a peak output voltage and the time at which the peak occurred.

The output voltage predicted by the model is the amplitude of the characteristic equation scaled according to the peak output voltage curve, with time scaled according to the driving current and flux capacity of the core. The descriptive equations for the Betts and Bishop model are extended to describe switching with an arbitrary driving current by

using a series of step driving currents to represent the arbitrary driving current and letting the time duration of each step approach zero. The Betts and Bishop model for an arbitrary driving current is

$$\left.\begin{aligned} V_{o,exp}(t) &= \begin{cases} 0 & (I_i(t) < I_{ext}) \\ R_p\left[I_i(t) - I_{ext}\right] f(\tau) & (I_i(t) \geqq I_{ext}) \end{cases} \\ \tau &= \begin{cases} 0 & (I_i(t) < I_{ext}) \\ \dfrac{R_p}{W_c} \displaystyle\int_{t_t}^{t} I_i(t)dt - I_{ext}(t - t_t) & (I_i(t) \geqq I_{ext}) \end{cases} \end{aligned}\right\} \quad (5)$$

The time at which the driving current reaches the threshold of the core is denoted by t_t.

The Nitzan Model

The Nitzan model predicts the output voltage of a thin core when completely switched, incompletely switched, and shuttled. A detailed description of the Nitzan model, which is only summarized in this report, is in reference 5. The model predicts the output voltage as the sum of the elastic switching component and the inelastic switching component:

$$V_{o,m} = \dot{\Phi}_{el} + \dot{\Phi}_{inel}$$

The elastic flux switched is the flux that will return to its initial value when the applied current is reduced to zero. The inelastic flux switched is the part of the total flux that will not return to its initial value when the driving current is reduced to zero. Inelastic switching produces the square hysteresis loop of a magnetic core.

The Nitzan model for elastic switching is

$$\dot{\Phi}_{el} = \epsilon \frac{dI_i(t)}{dt} \quad (6)$$

The slope of the static hysteresis loop in the saturated region is denoted by ϵ and is approximated by

$$\epsilon = \frac{\Phi_s - \Phi_r}{2\pi(r_o - r_i)H_a} \ln \frac{r_o}{r_i} \quad (7)$$

Only the elastic switching part of the Nitzan model is used to predict shuttling of the core.

The Nitzan model for inelastic switching is defined by the nonlinear differential equation

$$\dot{\Phi}_{inel}(t) = \dot{\Phi}_p(I)\left\{1 - \left[\frac{2\Phi(t) + \Phi_s - \Phi_{st}(I)}{\Phi_s + \Phi_{st}(I)}\right]^2\right\} \tag{8}$$

where $\dot{\Phi}_p(I)$ is the equation for peak output voltage as a function of amplitude of the step driving current, and $\Phi_{st}(I)$ is the equation describing the static hysteresis loop of the core. The static hysteresis loop is the relationship between current and flux of a magnetic core when switching as slowly as possible. Equation (8) was semiempirically derived by fitting a parabola to the relationship between voltage and flux of a magnetic core.

The equation of the static hysteresis loop $\Phi_{st}(I)$ is derived in such a way that it is represented by a set of parameters dependent on the core material and a set dependent only on the physical dimensions of the core. The advantage of having these two independent sets of parameters is that after experimentally testing one core and calculating the material parameters, the model can be applied to any core of this same material by merely adjusting the physical-dimension parameters in the model. The loop of flux density as a function of magnetic field intensity (B-H loop), from which the Φ-I loop is derived, depends only on the magnetic material. The B-H loop of the core being modeled is analytically described by hyperbolas as in figure B1. By means of the relationships

$$\Phi = \int B \cdot dA$$

and

$$I = \oint H \cdot d\ell$$

the equation describing the B-H loop for a material is converted to equations for the Φ-I loop for a core constructed of that material. The equations of the static Φ-I loop for a toroidal core are

$$\Phi_{st}(I) = \begin{cases} \dfrac{\Phi_s - \Phi_r}{(\ell_o - \ell_i)H_a} I \ln \dfrac{I - H_a\ell_o}{I - H_a\ell_i} - \Phi_r & (I \leq I_{st}) \\ \dfrac{(\Phi_s + \Phi_r)H_q}{(\ell_o - \ell_i)H_n}\left[\dfrac{I}{H_q} - \ell_i + I\left(\dfrac{1}{H_n} - \dfrac{1}{H_q}\right) \ln \dfrac{1 - \dfrac{H_n}{H_q}}{\dfrac{H_n\ell_i}{I}}\right] - \Phi_r & (I_{st} < I < H_q\ell_o) \\ \dfrac{(\Phi_s + \Phi_r)H_q}{(\ell_o - \ell_i)H_n}\left[\ell_o - \ell_i + I\left(\dfrac{1}{H_n} - \dfrac{1}{H_q}\right) \ln \dfrac{I - H_n\ell_o}{I - H_n\ell_i}\right] - \Phi_r & (H_q\ell_o \leq I) \end{cases} \tag{9}$$

By using experimental data which describe the static hysteresis loop and the dimensions of the core, a computer program fits equation (9) to the Φ-I loop data by adjusting H_a, H_q, and H_n, which are material parameters.

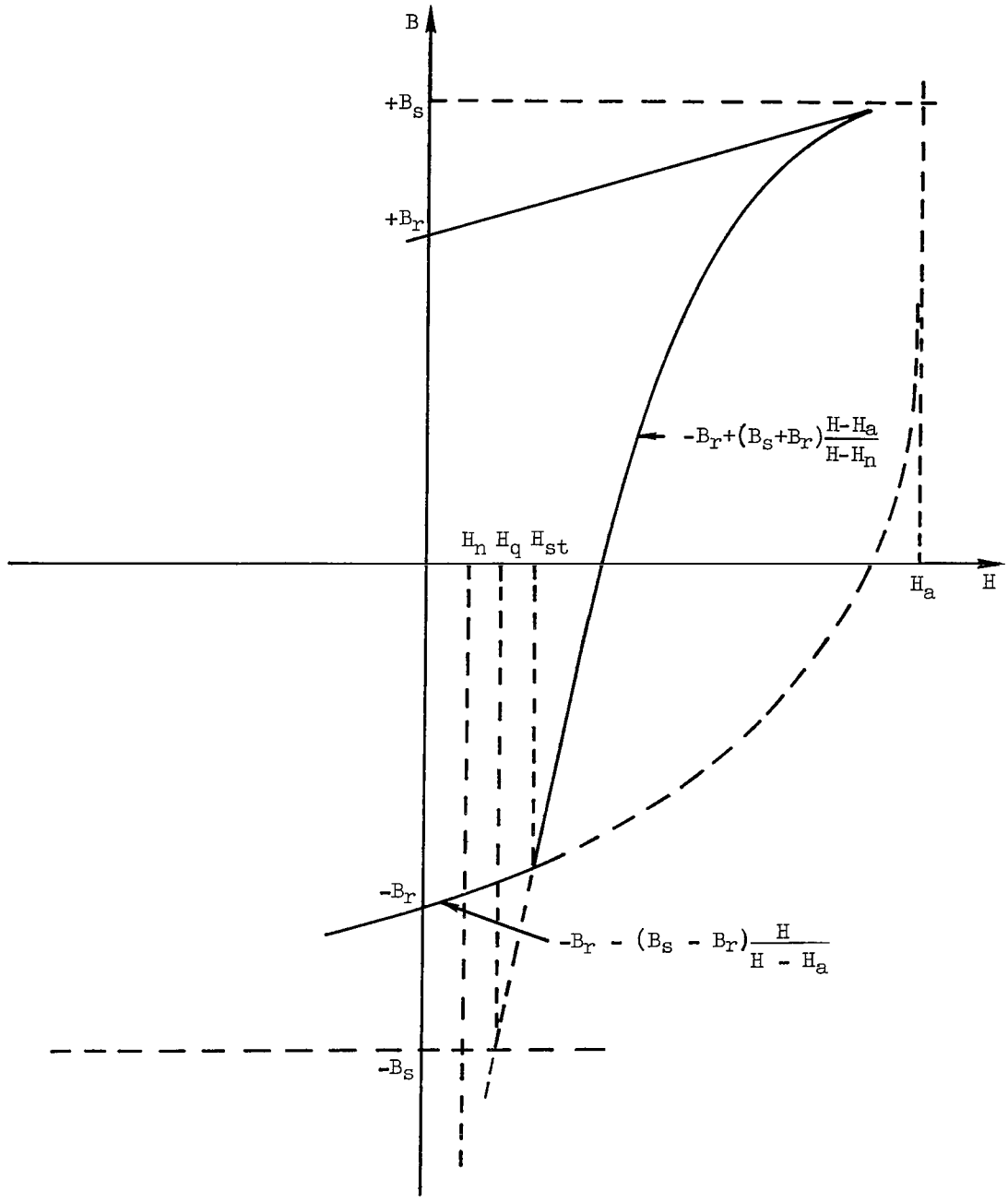

Figure B1.- Static B-H loop.

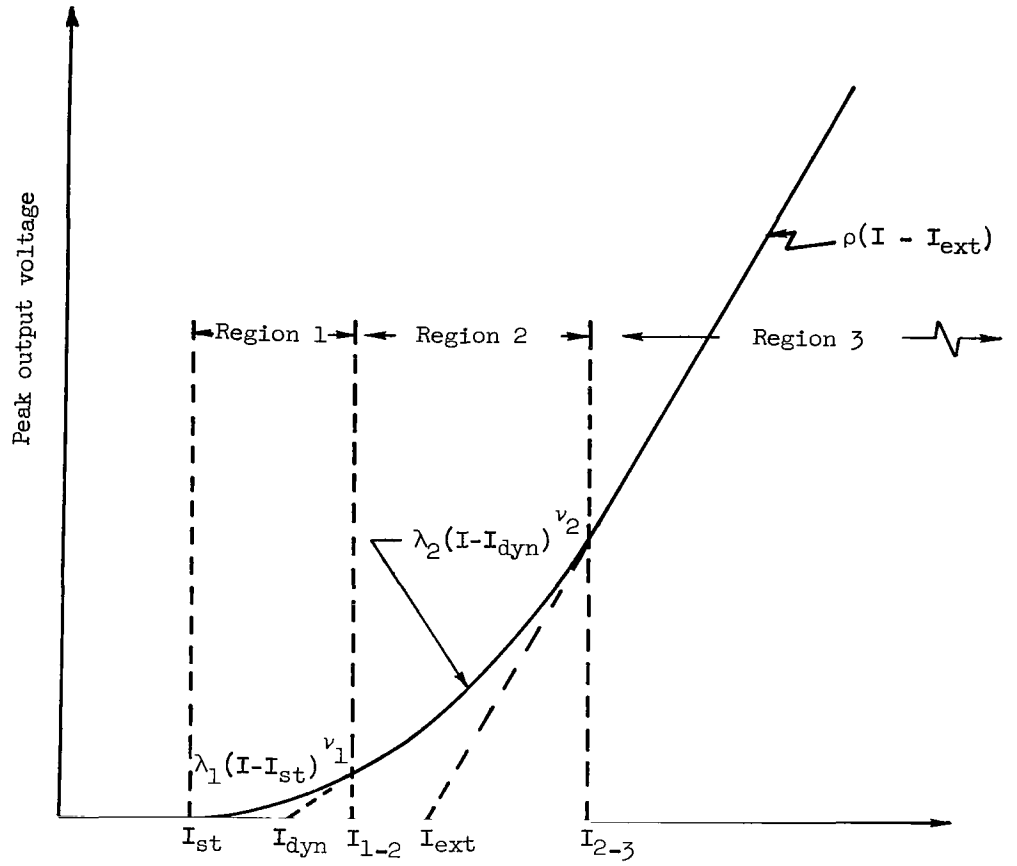

Figure B2.- Peak output voltage curve with regions.

The relationship of peak output voltage to amplitude of step driving current is shown in figure B2. The curve is divided into two nonlinear regions and one linear region. The equations describing the regions are as follows:

$$\dot{\Phi}_p(I) = \begin{cases} 0 & \left(0 \leqq I < I_{st}\right) \\ \lambda_1\left(I - I_{st}\right)^{\nu_1} & \left(I_{st} \leqq I < I_{1-2}\right) \\ \lambda_2\left(I - I_{dyn}\right)^{\nu_2} & \left(I_{1-2} \leqq I < I_{2-3}\right) \\ \rho\left(I - I_{ext}\right) & \left(I_{2-3} \leqq I\right) \end{cases} \tag{10}$$

A computer program fits equations (10) to the experimental peak output voltage data by adjusting λ_1, λ_2, ν_1, ν_2, ρ, I_{ext}, I_{dyn}, and I_{st}. If the core is assumed to be a thin toroid, the material parameters of the core are determined by use of the following equations:

$$H_{dyn} = \frac{I_{dyn}}{\bar{l}} \qquad \delta = \frac{\bar{l}}{h(r_o - r_i)}\rho$$

$$H_{2-3} = \frac{I_{2-3}}{\bar{l}} \qquad B_s = \frac{\Phi_s}{h(r_o - r_i)}$$

$$H_{ext} = \frac{I_{ext}}{\bar{l}} \qquad B_r = \frac{\Phi_r}{h(r_o - r_i)}$$

$$H_{st} = \frac{I_{st}}{\bar{l}} \qquad \kappa_2 = \frac{\bar{l}^{\nu_2}}{h(r_o - r_i)}\lambda_2$$

$$H_{1-2} = \frac{I_{1-2}}{\bar{l}} \qquad \kappa_1 = \frac{\bar{l}^{\nu_1}}{h(r_o - r_i)}\lambda_1$$

The parameters H_{dyn}, H_{2-3}, H_{ext}, H_{st}, H_{1-2}, δ, B_s, B_r, κ_2, and κ_1 are material parameters.

Because of the complexity of the peak output voltage equations (10) and static hysteresis loop equations (9), the descriptive equation (8) must be solved numerically on a digital computer. An arbitrary driving current is represented by a series of step driving currents of very small time duration, and a simple predictor-corrector method is used to solve equation (8) for $\dot{\Phi}_{inel}(t)$. By summing $\dot{\Phi}_{inel}$ and $\dot{\Phi}_{el}$, the total output voltage of a core driven by an arbitrary drive current is predicted by the Nitzan model.

REFERENCES

1. Menyuk, N.; and Goodenough, J. B.: Magnetic Materials for Digital-Computer Components. I. A Theory of Flux Reversal in Polycrystalline Ferromagnetics. J. Appl. Phys., vol. 26, no. 1, Jan. 1955, pp. 8-18.

2. Hesterman, V. W.: Evaluation of Flux-Switching Models for Magnetic Devices. Tech. Rep. 2 (Contract Nonr 2712(00)), Stanford Res. Inst., Sept. 1961. (Available from DDC as AD 263 623.)

3. Nitzan, D.: Flux Switching in Multipath Cores. Rep. 1 (Contracts NASw-6 and JPL-950095), Stanford Res. Inst., Nov. 1961.

4. Nitzan, D.; and Hesterman, V. W.: Flux Switching in Multipath Cores. Rep. 2 (Contracts NASw-6 and JPL-950095), Stanford Res. Inst., Nov. 1962.

5. Nitzan, D.; and Hesterman, V. W.: Flux Switching in Multipath Cores. Rep. 3 (Contracts NASw-6 and JPL-950095), Stanford Res. Inst., June 1964.

6. Nitzan, D.; and Hesterman, V. W.: Flux Switching in Multipath Cores. Rep. 4 (Contracts NAS7-100 and JPL-950943), Stanford Res. Inst., July 1965.

7. Nitzan, D.; Hesterman, V. W.; and Van De Riet, E. K.: Flux Switching in Magnetic Circuits. Rep. 5 (Contracts NAS7-100 and JPL-951383), Stanford Res. Inst., Nov. 1966.

8. Nitzan, D.: Engineering Flux-Switching Models for Toroidal and Multipath Cores. IEEE Trans. Communic. and Electron., vol. CE-83, no. 72, May 1964, pp. 309-314.

9. Nitzan, David: Computation of Flux Switching in Magnetic Circuits. IEEE Trans. Magnetics, vol. MAG-1, no. 3, Sept. 1965, pp. 222-234.

10. Nitzan, David: Models for Elastic and Inelastic Flux Switching. IEEE Trans. Magnetics, vol. MAG-2, no. 4, Dec. 1966, pp. 751-760.

11. Betts, R.; and Bishop G.: Ferrite Toroid Core Circuit Analysis. IRE Trans. Electron. Computers, vol. EC-10, no. 1, Mar. 1961, pp. 51-56.

12. Spencer, John Larry: The Evaluation of Two Flux-Switching Models for Magnetic Cores. M.S. Thesis, Virginia Polytech. Inst., 1969.

13. Anon.: Final Report on the Development and Use of Multiaperture-Core Flux Logic Devices to Perform Logical Functions in Digital Data Processing. Vol. I. WADC-TR-59-648, U.S. Air Force, Dec. 1959. (Available from DDC as AD 231 176.)

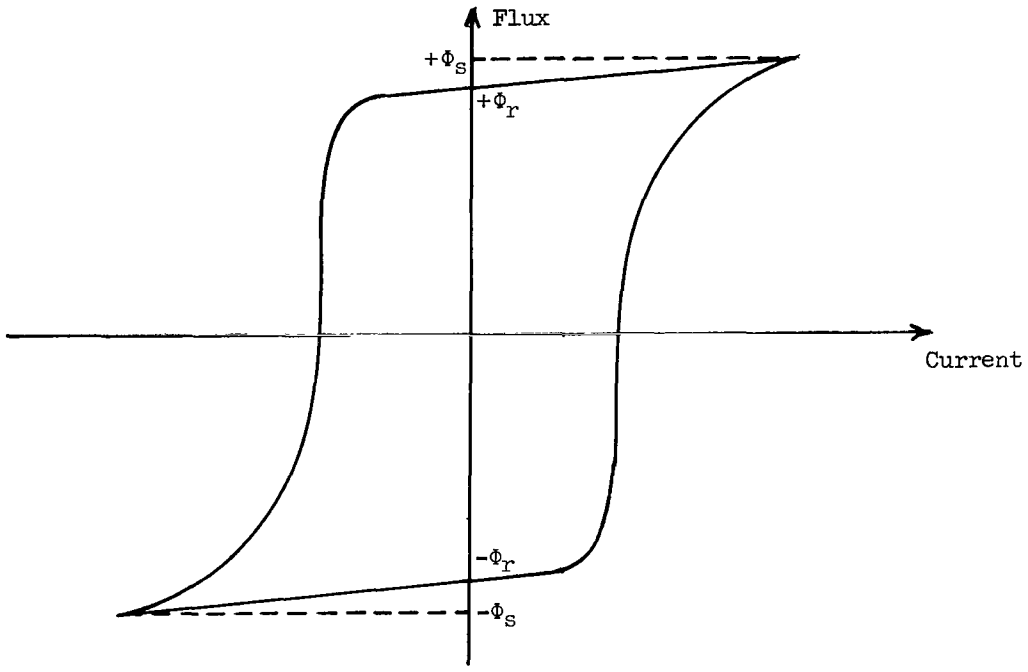

Figure 1.- Typical hysteresis loop for a magnetic core.

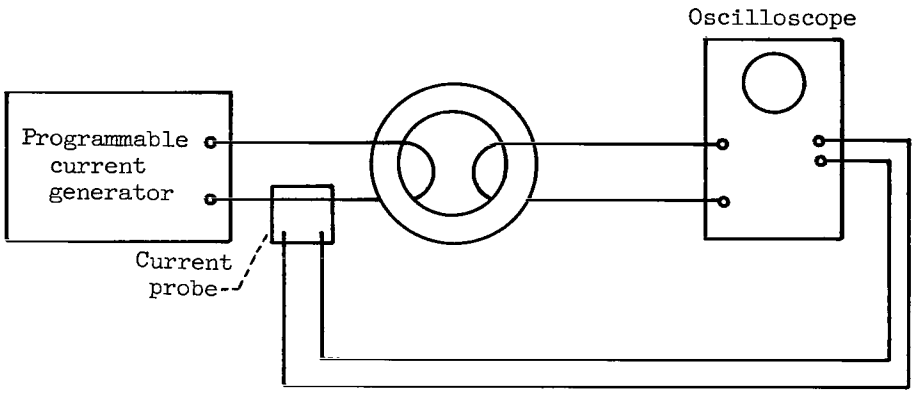

Figure 2.- Test circuit.

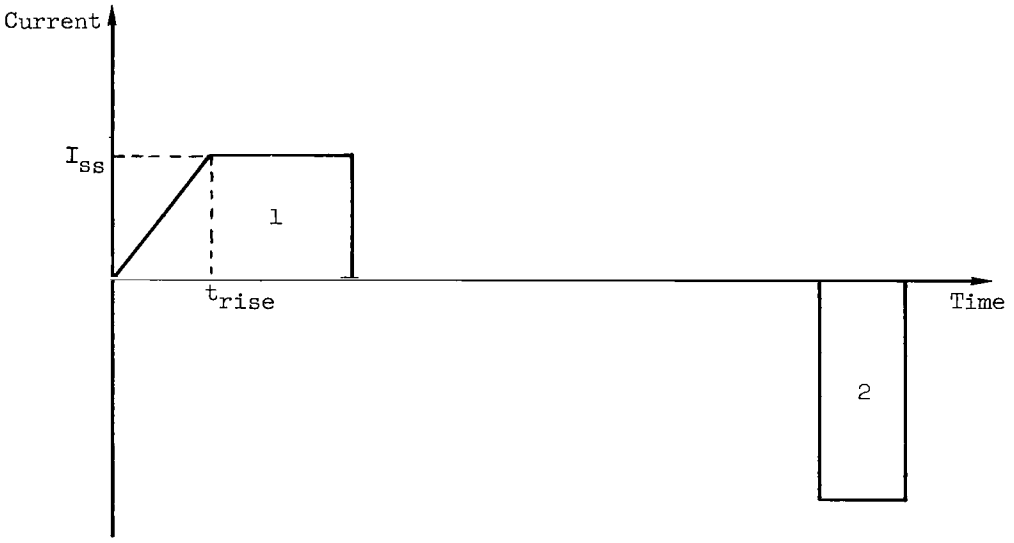

Figure 3.- Pulse sequence from the pulse generator of figure 2.

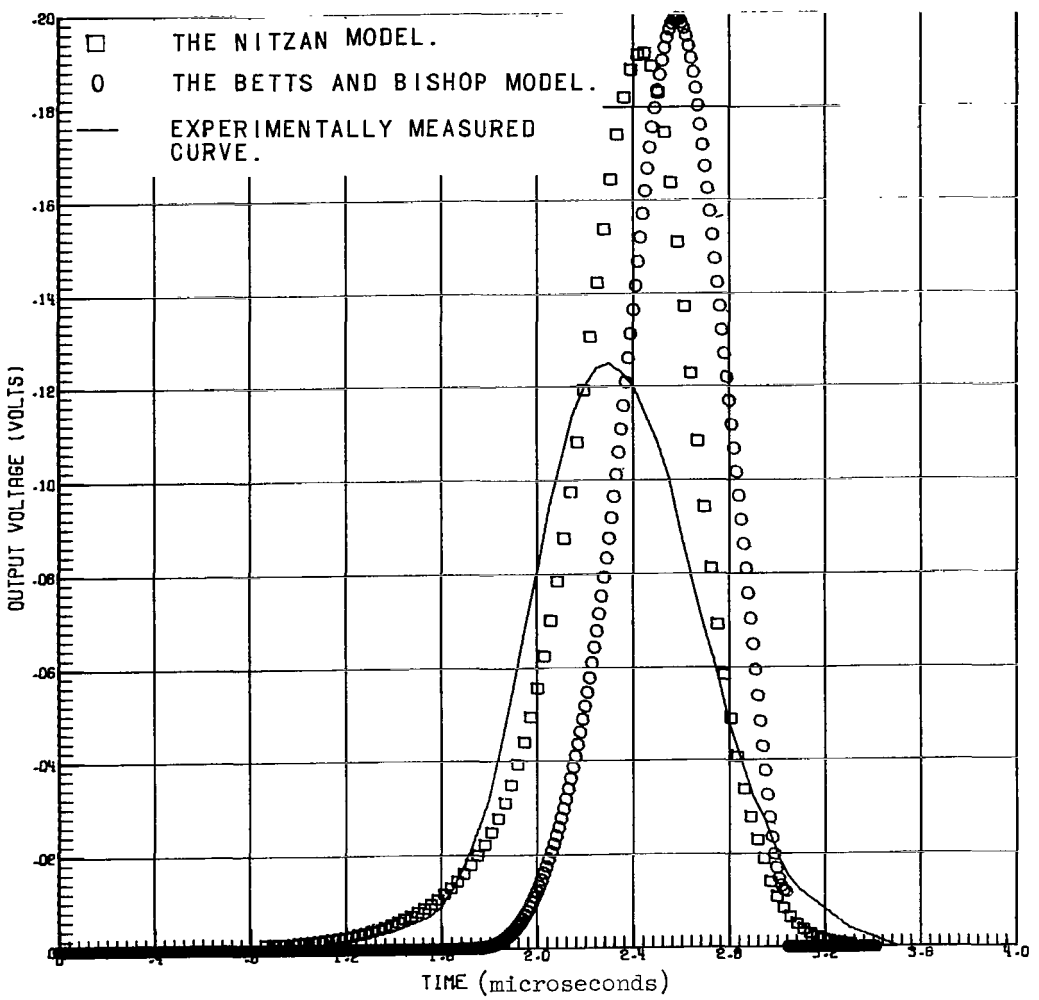

Figure 4.- Output voltage for ramp switching.

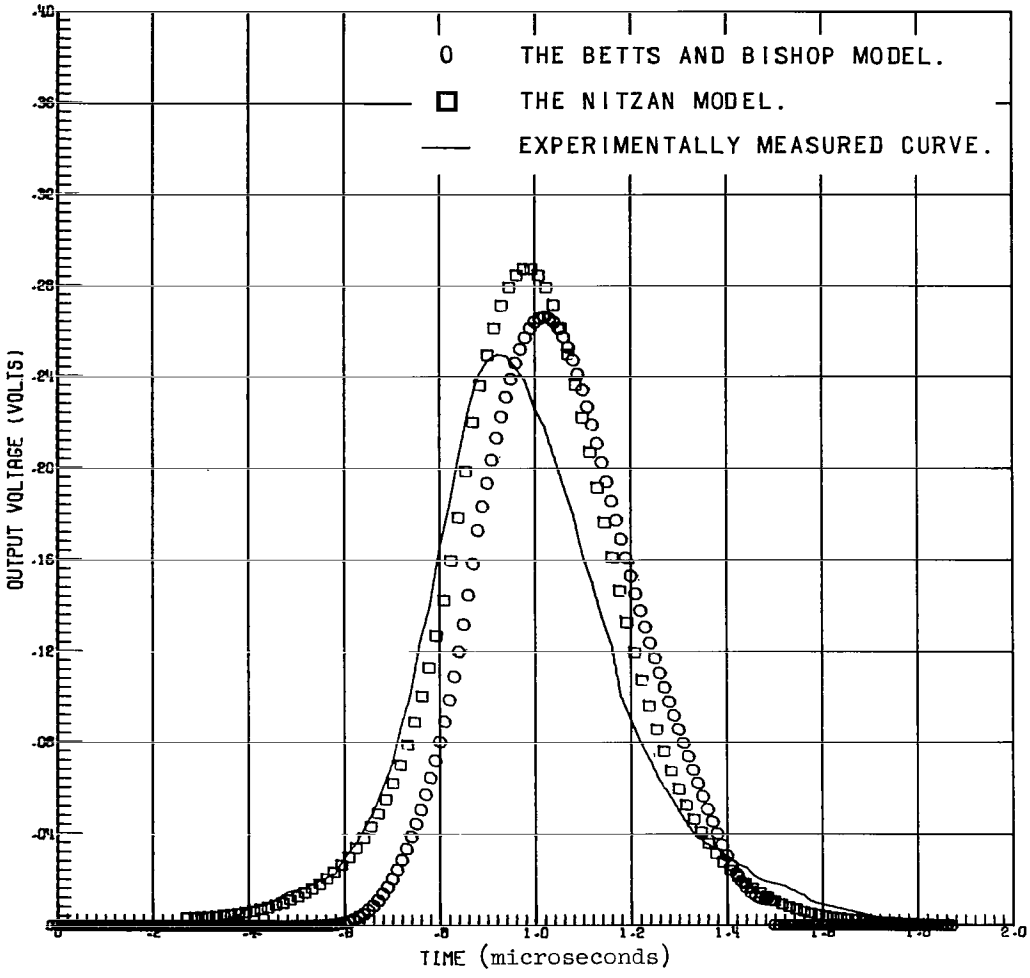

Figure 5.- Output voltage for ramp-step switching.

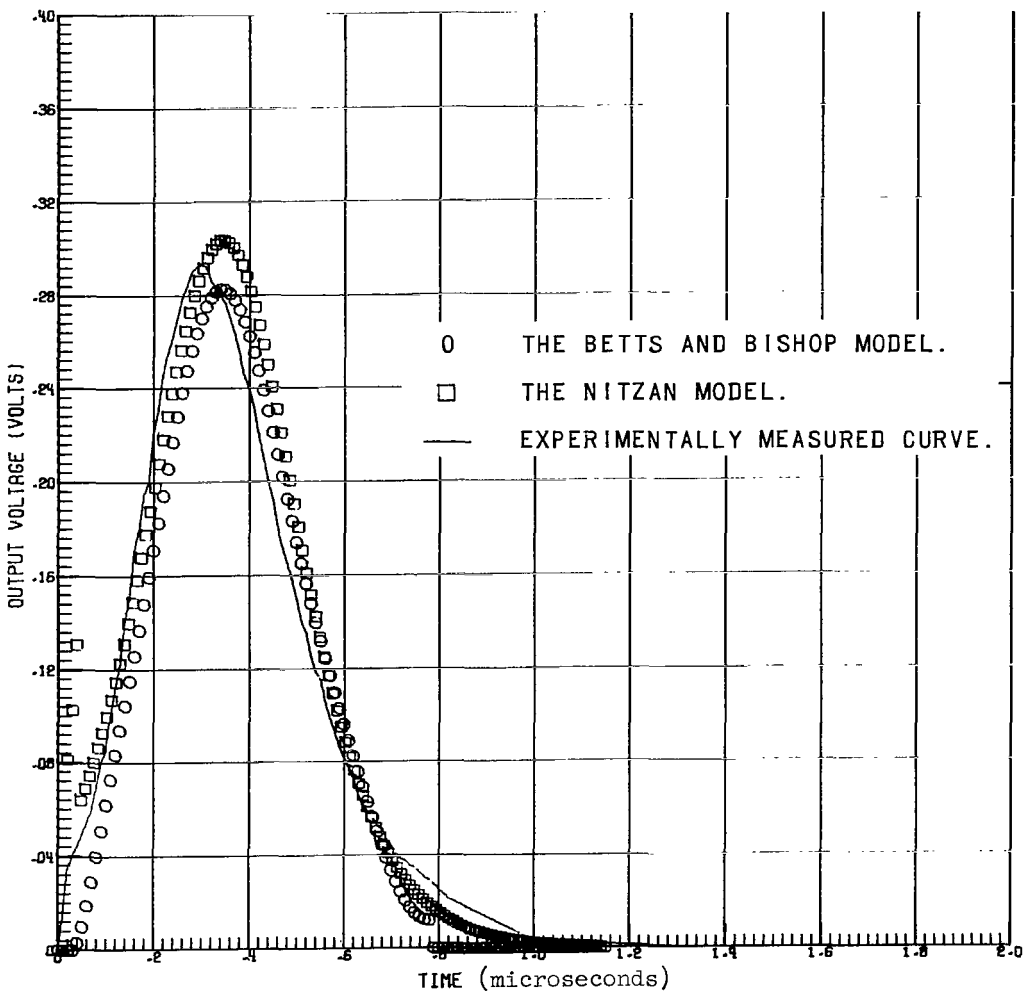

Figure 6.- Output voltage for slow step switching.

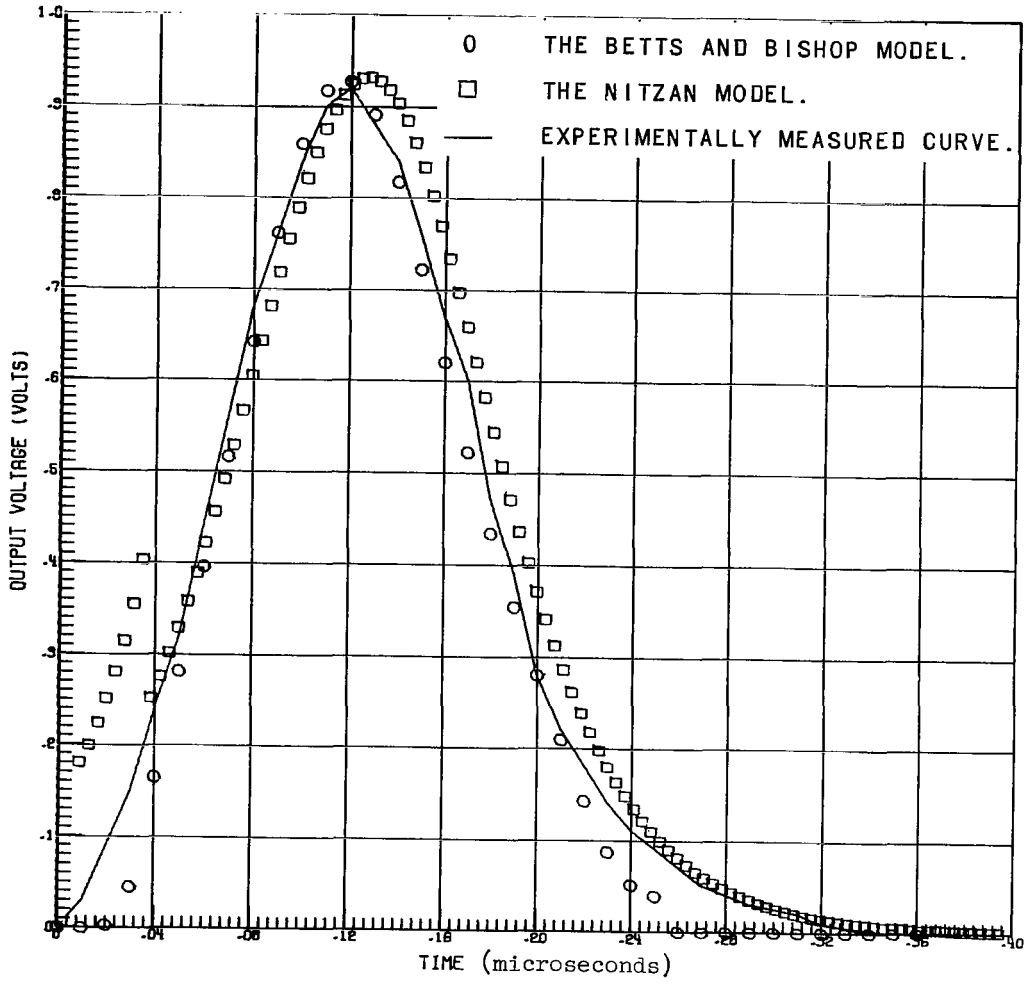

Figure 7.- Output voltage for fast step switching.

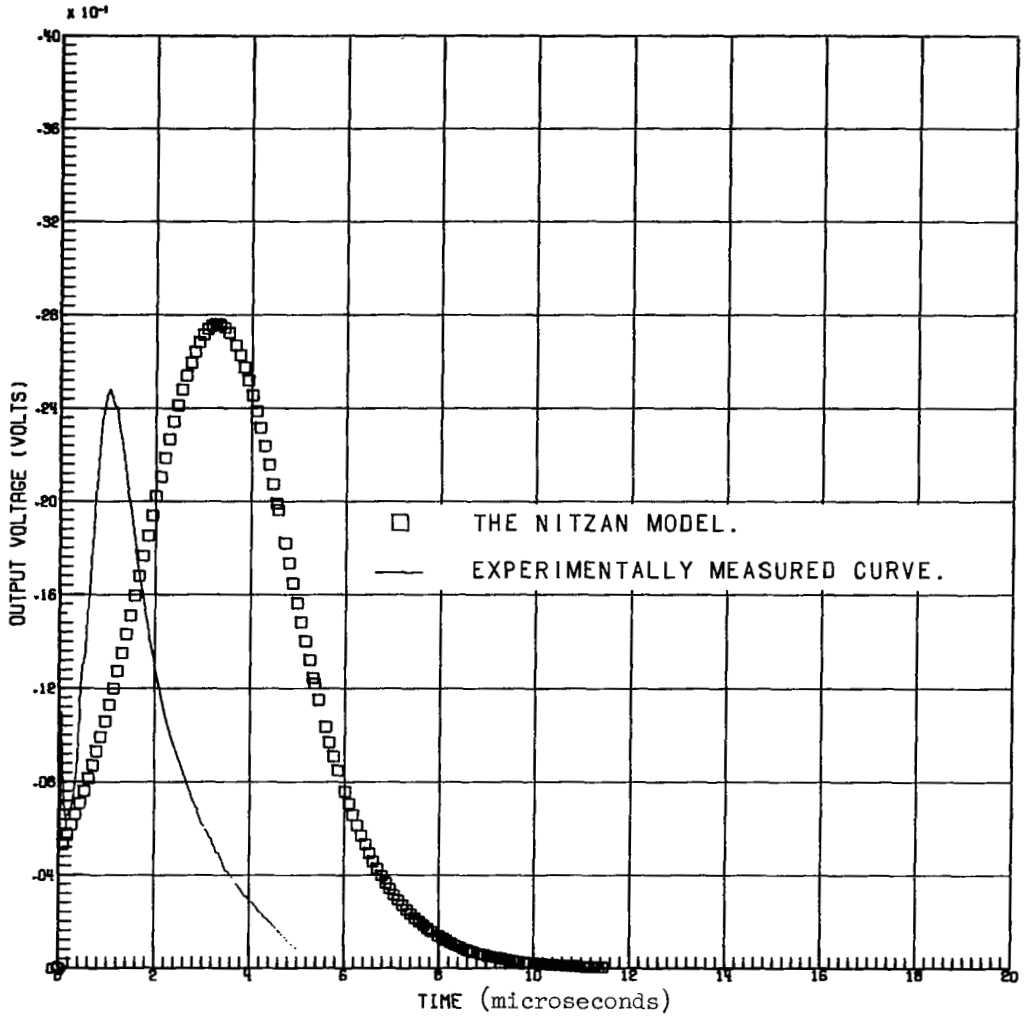

Figure 8.- Output voltage of partially switched core.

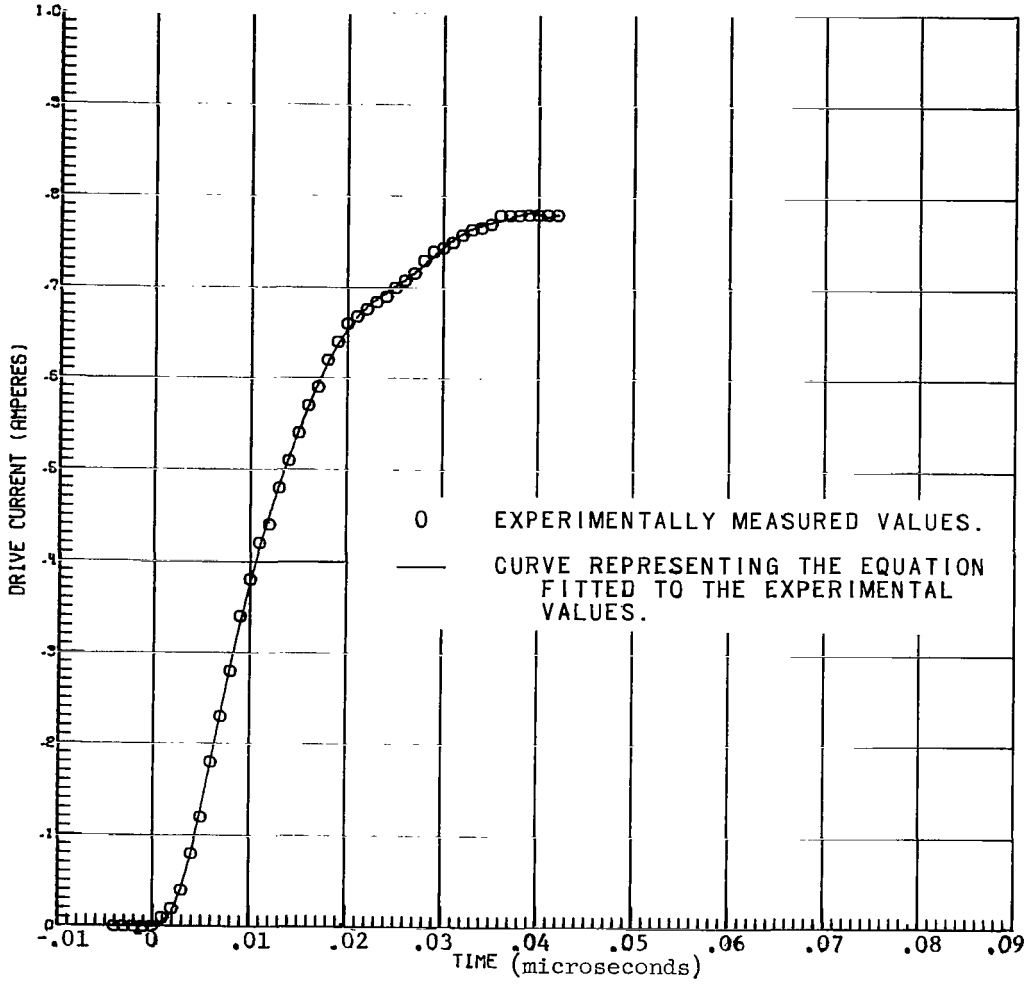

Figure 9.- Driving current for shuttling the core.

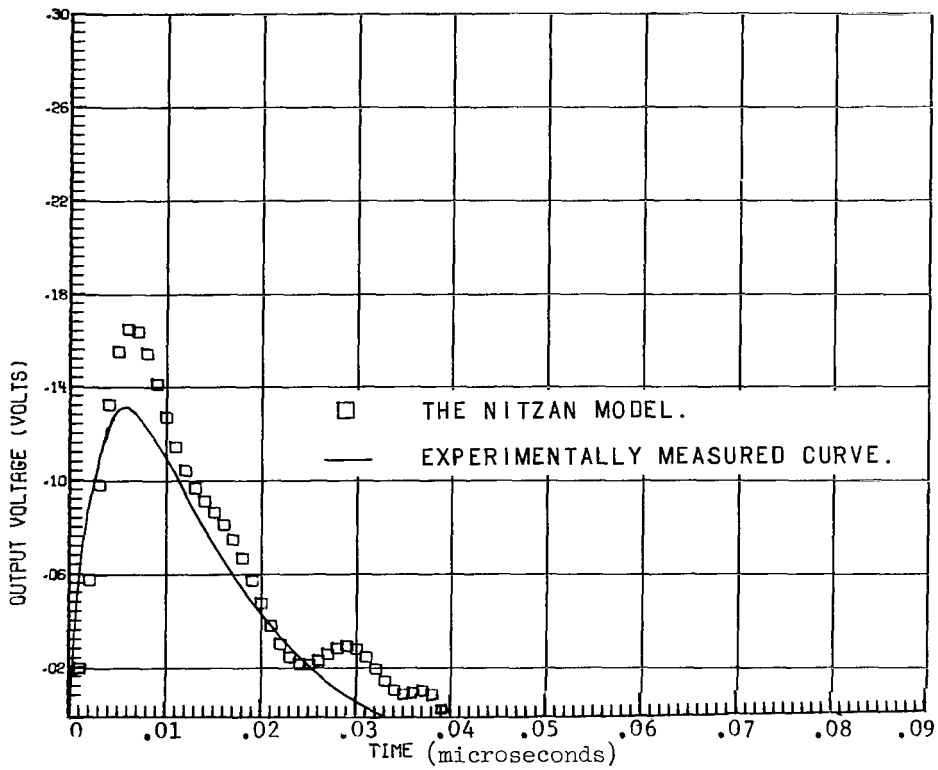

Figure 10.- Shuttling output voltage.

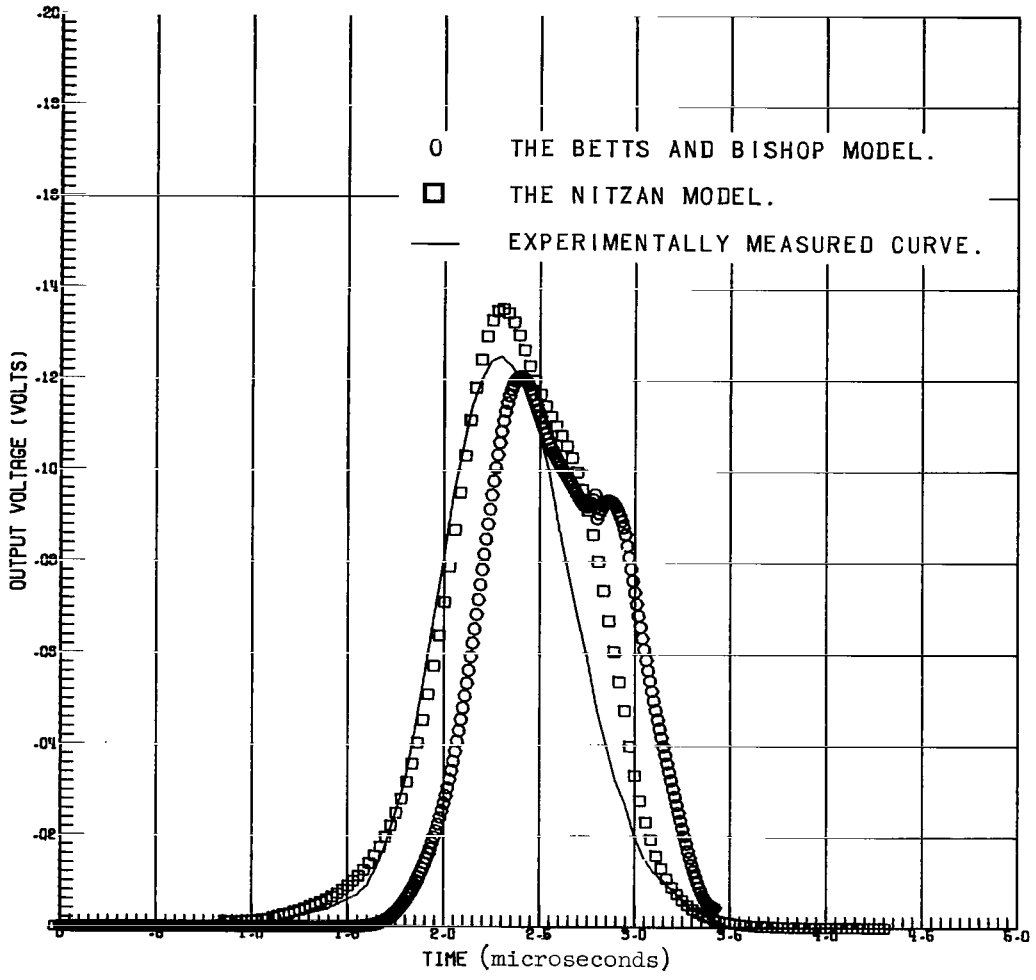

Figure 11.- Output voltage of ramp switching with two rings.

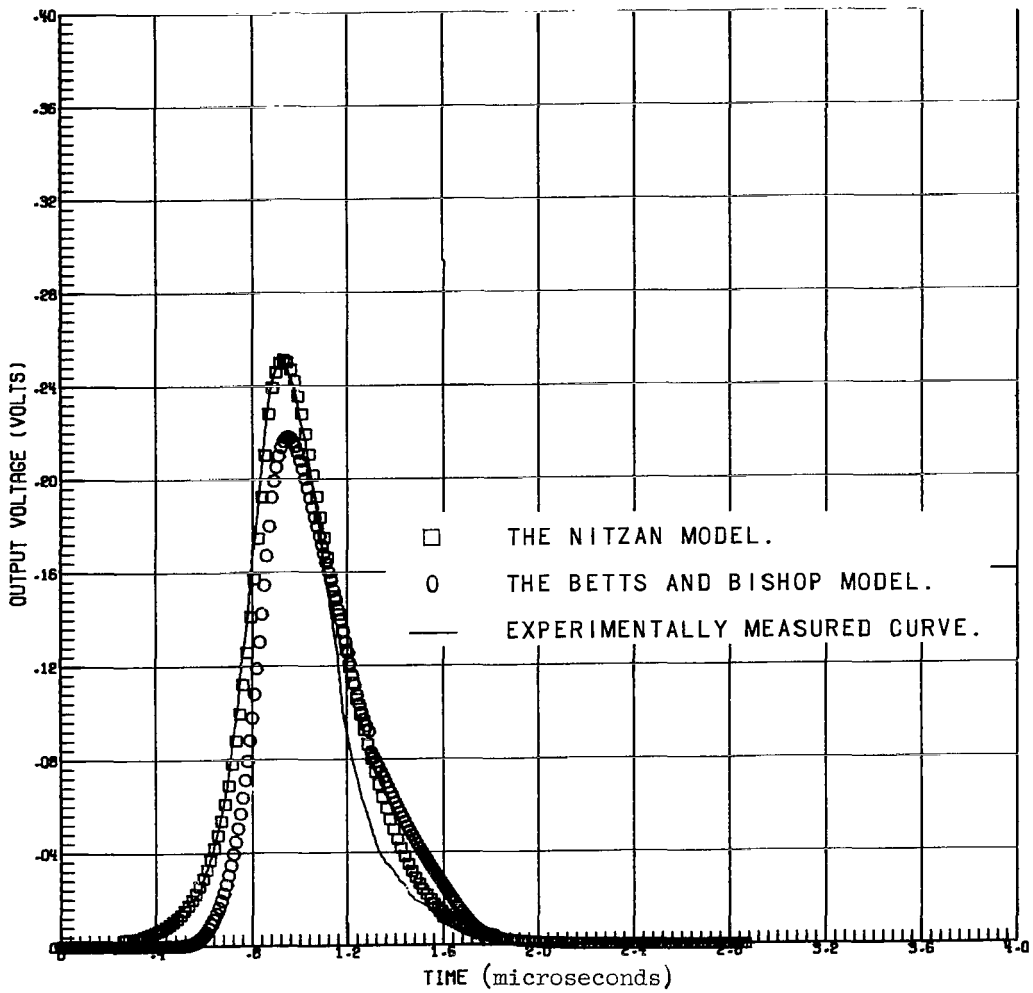

Figure 12.- Output voltage of ramp-step switching with two rings.

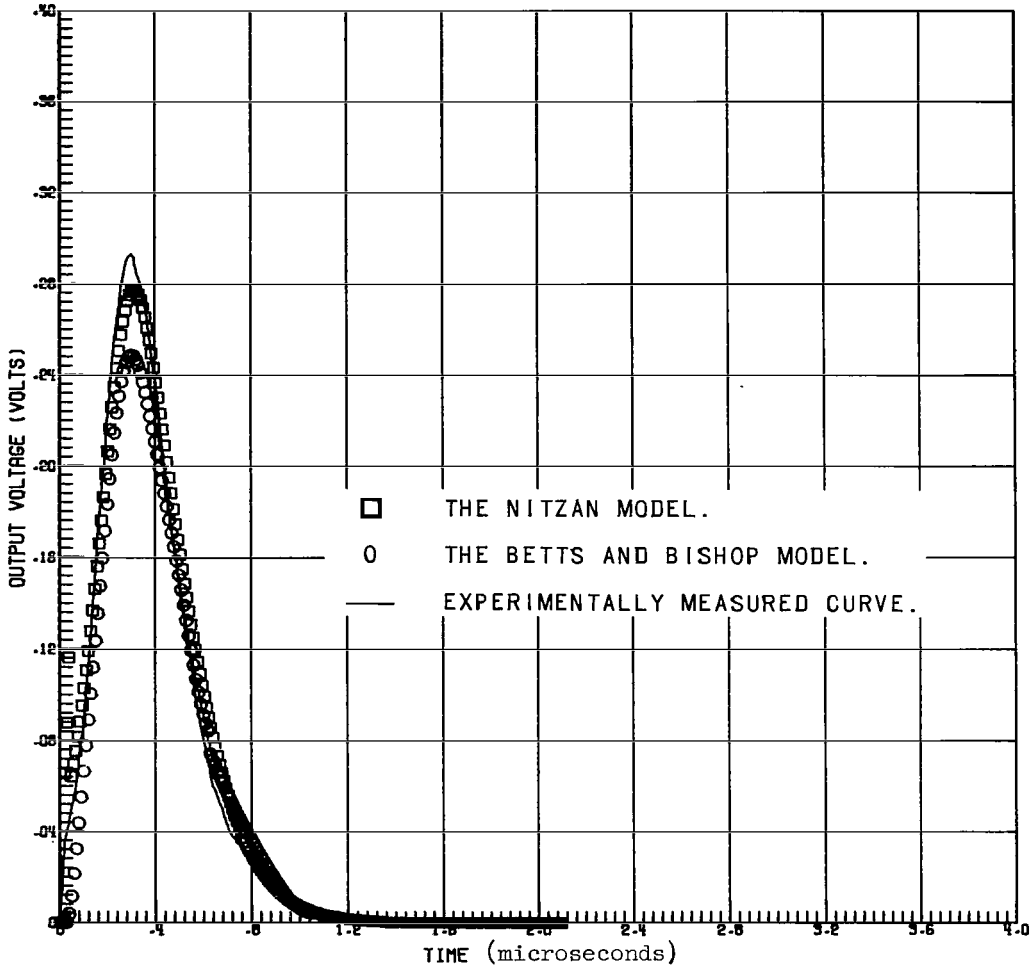

Figure 13.- Output voltage of slow step switching with two rings.

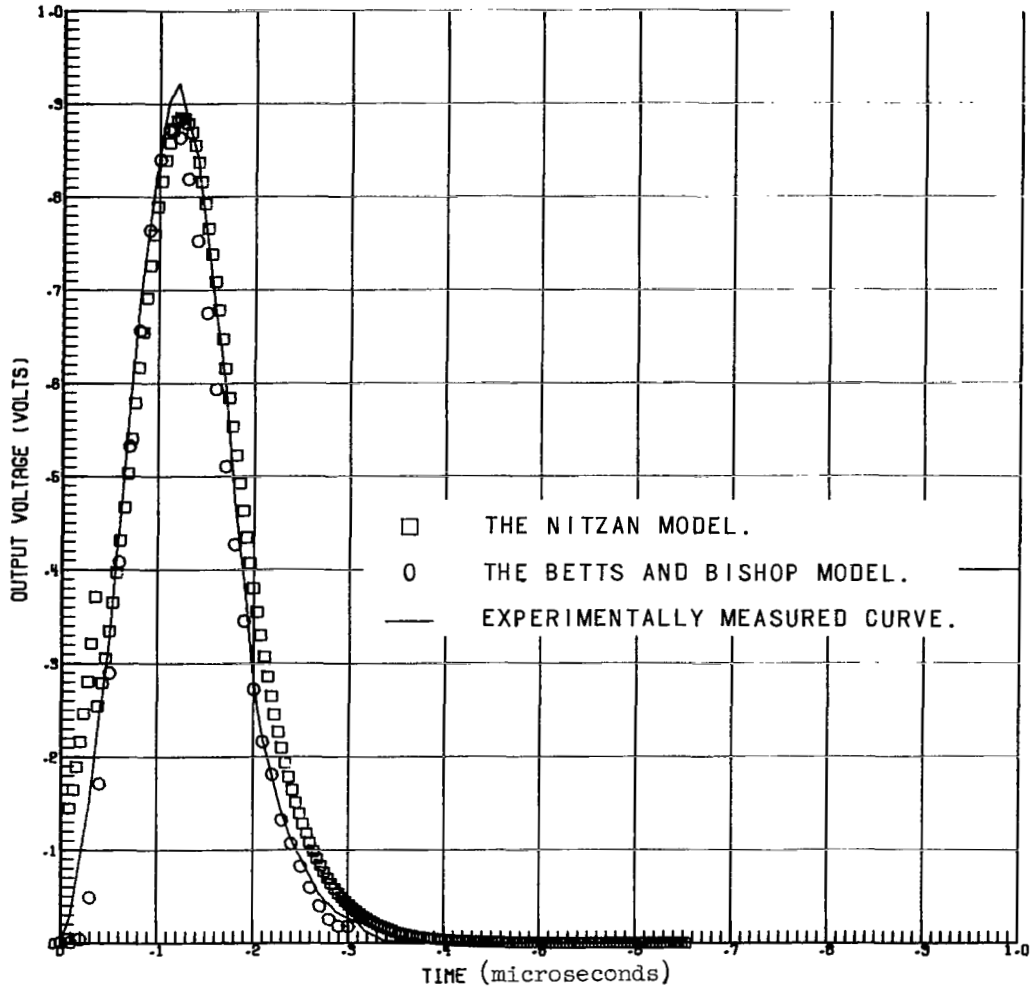

Figure 14.- Output voltage of fast step switching with two rings.

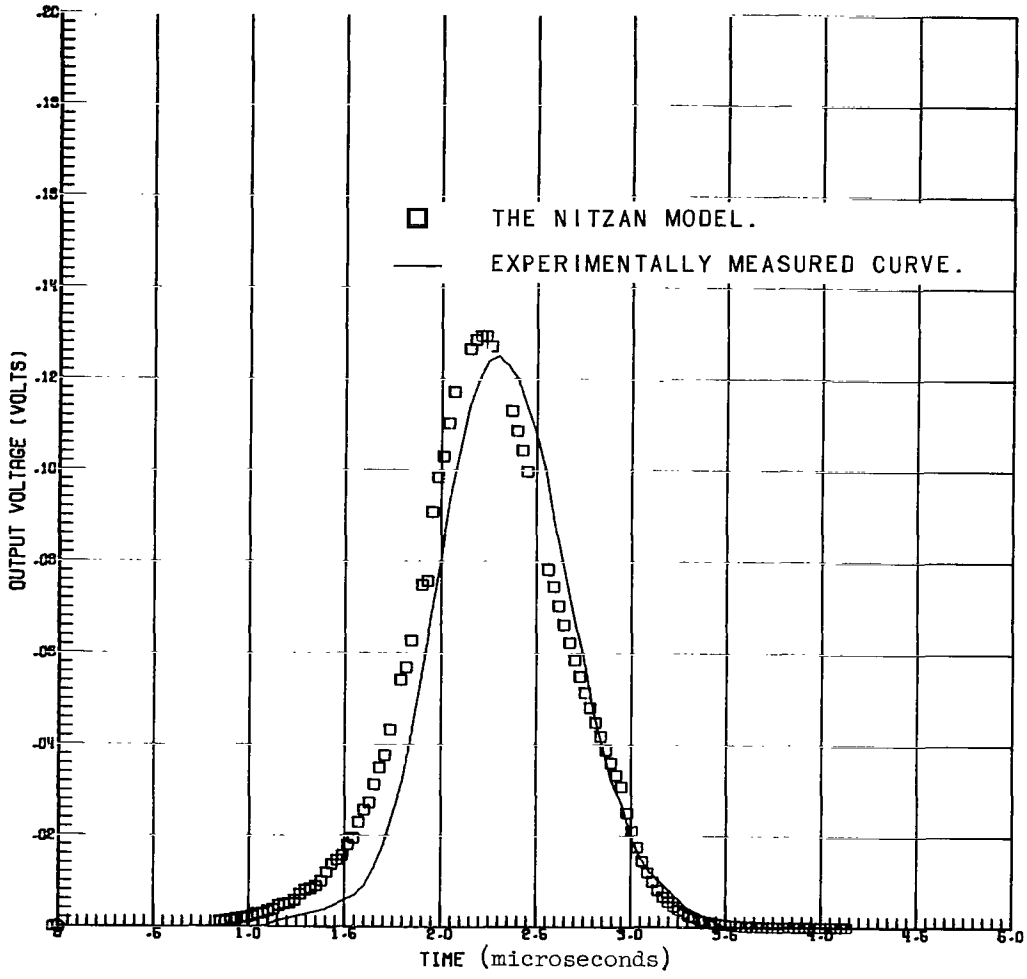

Figure 15.- Output voltage of ramp switching with 10 rings.

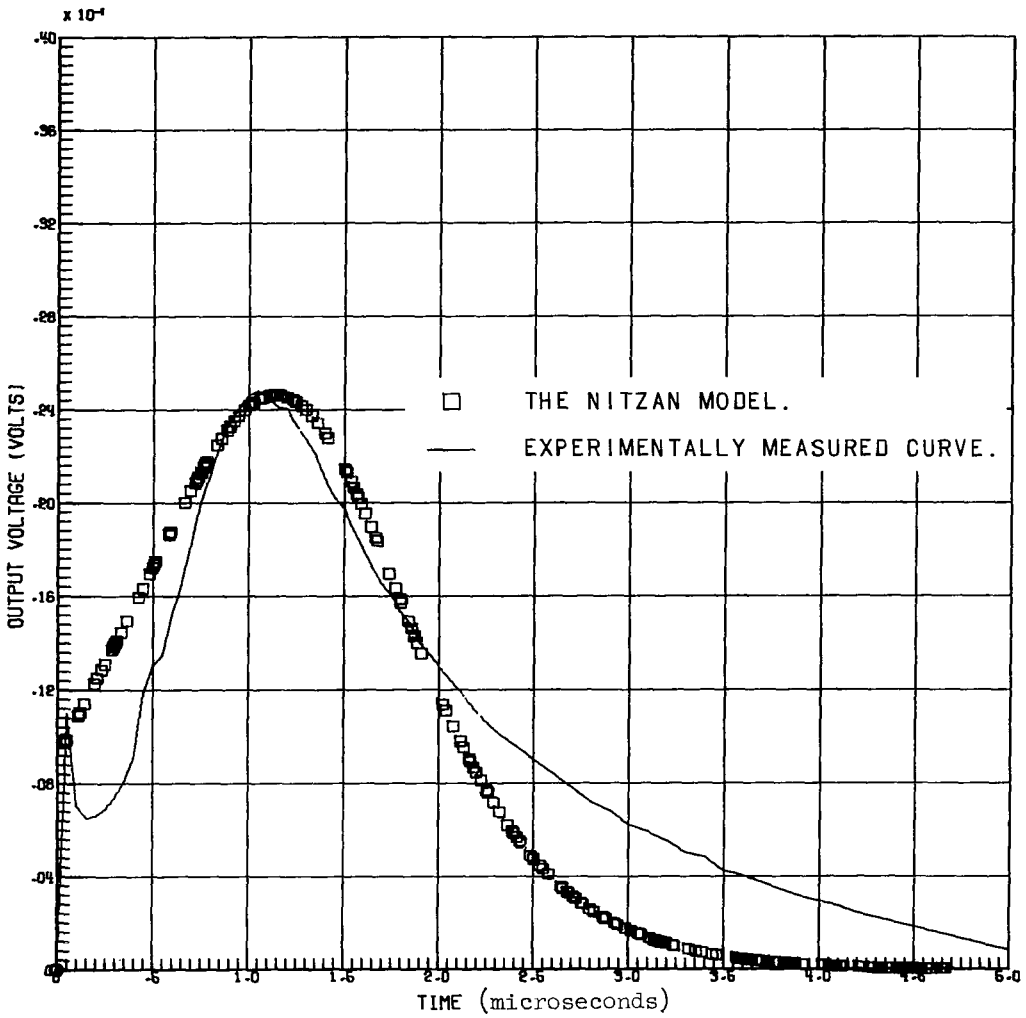

Figure 16.- Output voltage of partially switched core with 10 rings.

NASA-Langley, 1970 —— 10 L-7300

06U 001 44 51 3DS 70286 00903
AIR FORCE WEAPONS LABORATORY /WLOL/
KIRTLAND AFB, NEW MEXICO 87117

ATT E. LOU BOWMAN, CHIEF,TECH. LIBRARY

"The aeronautical and space activities of the United States shall be conducted so as to contribute . . . to the expansion of human knowledge of phenomena in the atmosphere and space. The Administration shall provide for the widest practicable and appropriate dissemination of information concerning its activities and the results thereof."

—NATIONAL AERONAUTICS AND SPACE ACT OF 1958

NASA SCIENTIFIC AND TECHNICAL PUBLICATIONS

TECHNICAL REPORTS: Scientific and technical information considered important, complete, and a lasting contribution to existing knowledge.

TECHNICAL NOTES: Information less broad in scope but nevertheless of importance as a contribution to existing knowledge.

TECHNICAL MEMORANDUMS: Information receiving limited distribution because of preliminary data, security classification, or other reasons.

CONTRACTOR REPORTS: Scientific and technical information generated under a NASA contract or grant and considered an important contribution to existing knowledge.

TECHNICAL TRANSLATIONS: Information published in a foreign language considered to merit NASA distribution in English.

SPECIAL PUBLICATIONS: Information derived from or of value to NASA activities. Publications include conference proceedings, monographs, data compilations, handbooks, sourcebooks, and special bibliographies.

TECHNOLOGY UTILIZATION PUBLICATIONS: Information on technology used by NASA that may be of particular interest in commercial and other non-aerospace applications. Publications include Tech Briefs, Technology Utilization Reports and Notes, and Technology Surveys.

Details on the availability of these publications may be obtained from:

SCIENTIFIC AND TECHNICAL INFORMATION DIVISION

NATIONAL AERONAUTICS AND SPACE ADMINISTRATION

Washington, D.C. 20546